(Submitted to *Journal* of Guidance, Control, and Dynamics)

Optimization Methods for Passive Damper Placement and Tuning

Mark H. *Milman*[1] and *Cheng-Chih Chu*[2]

MS 198-326

Jet Propulsion Laboratory

California *Institute* of Technology

4800 Oak Grove Drive

Pasadena, CA *91109*

Submitted: *July* 21, 1992

Revised: May 5, 1993

[1] Member of Technical Staff, Guidance and Control Section

[2] Member of Technical Staff, Guidance and *Control* Section

Abstract

The effectiveness of viscous elements in introducing damping in a structure is a function of several variables, including their number, their location in the structure, and their physical properties. This paper addresses the questions of the placement of these elements and the selection of their physical parameters via optimization techniques. The paper investigates various metrics to define these optimization problems, and compares the damping profiles that are obtained. Both discrete and continuous optimization problems are formulated and solved, corresponding, respectively, to the problems of placement of damping elements and to the tuning of their parameters. Particular emphasis is placed on techniques to make feasible the large scale problems resulting from the optimization formulations. Numerical results involving a lightly damped testbed structure are presented.

1. Introduction

A problem of considerable importance in the development of technology for future space structures is the analysis and optimization of passive elements placed in these structures. Passive damping introduced by these devices is an effective mechanism for reducing peak responses in the vicinity of resonant frequencies for lightly damped systems, This not only enhances the stability of the open loop system, but also allows for the implementation of more aggressive control strategies to achieve greater performance. This philosophy is being pursued on a series of Control Structure Interaction (CSI) testbeds at the Jet Propulsion Laboratory.

The effectiveness of viscous elements in introducing damping is a function of several variables, including their number, their location in the structure, and their physical parameters. This paper is concerned with the problems of the placement and tuning of the damping parameters with particular emphasis on techniques to make feasible the numerical solution of the large scale problems associated with the optimization of these variables. Two qualitatively different optimization problems are considered in the paper: a combinatorial optimization problem is posed to determine the placement of elements, and a mathematical programming

problem is posed to optimize the damper parameters. A simulated annealing strategy [6] is used for the combinatorial optimization problem, while a sequential quadratic programming algorithm (SQP) [2] is applied to the damper parameter optimization problem. The question of developing a hybrid approach for combining these strategies into a single approach is not taken up in the present paper, and the primary focus here is on how to solve each of these problems individually.

TWO different metrics are developed for the optimization. The first metric measures damping in selected modes. In practice these modes would be chosen. based on their participation in particular transfer functions and their frequencies (e.g., at loop gain crossover). The second metric is the $\mathcal{H}_2$ norm of selected transfer functions of interest. These would typically be between disturbance inputs and measured or controlled outputs.

Fundamental ingredients in any optimization solution are the cost functional evaluation and the determination of search direction. Regardless of the metric that is used, these evaluations arc especially challenging problems here due to the size of the system. (The JPL testbed is modeled with approximately 250 degrees–of–freedom.) An efficient Newton's method that exploits the small rank perturbations to the nominal stiffness matrix introduced by the insertion of damping elements is developed for function evaluation of the damping metric. In a similar manner an eigenvector update technique that also uses a small rank perturbation approach leads naturally to an analytic gradient evaluation of the damping metric which circumvents the need for the costly finite difference approximations that are necessary for deriving a search direction in the parameter optimization problem. The Newton algorithm with the analytical gradient calculation produces a very efficient implementation of the SQP algorithm for this optimization problem. The $\mathcal{H}_2$ metric requires solving a large order Lyapunov equation. Here a Ritz reduction method that has been studied in [1] is employed to reduce the numerical bottleneck created by solving large systems of this type. Yiu [10] has also utilized this reduction method in analyzing the system level behavior of dampers in structures. In [9] a '(time–domain" energy metric is used to optimize the placement of dampers.

The problem addressed in this paper can be viewed as a very specialized version of the general

design problem of simultaneous placement of sensors and actuators, and selection of control gains. The damper placement and tuning problem focuses this more general problem to a very specific architecture – collocated actuator and sensors, and a diagonal multivariable position and velocity feedback structure. Various aspects of this general problem have been taken up, for example, in [9],[13],[14],[15]. The article [13] seeks to optimally place actuators for static alignment and shape control, and employs a heuristic integer programming programming algorithm for finding the placements. In [14] and [15] combined actuator and sensor placement is addressed by successive deletion of actuators" and sensors that contribute least to closed loop performance. In [9] a '(time-domain" energy metric is used in conjunction with simulated annealing to place dampers in a truss structure. Other aspects of this problem are taken up in for example [11], [12], [16], [17], [18].

A brief outline of the paper follows. The second section introduces the general problem formulation. This includes the modeling of the mechanical system with damping elements, the definition of the design space, and the type of cost functional and optimization problems that will be addressed in the remainder of the paper. Section 3 is concerned with functional and gradient evaluation for a class of damping functional. The Newton algorithm for the functional evaluation is developed as well as an algorithm for computing the damping functional gradient map. In the fourth section the H_2 metric cost functional is introduced, and the Ritz reduction method for approximating the calculation of this cost objective is discussed. in the fifth section several example problems involving the JPL Phase B testbed are solved. The efficacy of the computational techniques are illustrated as well as some pitfalls associated with using a modal truncation approach as an approximation technique for computing damping values. The examples demonstrate that optimizing appropriate cost functional is an effective method for selecting damper placement and tuning parameters to tailor structural response.

2. Problem Definition

We begin with the model of the system. Assume that the nominal structure is undamped and r dampers are added to the system. (The number of dampers is fixed throughout this paper.) Each damper is modeled as a collocated position plus velocity feedback control element with

gains k_p^i and k_v^i, respectively, for $i = 1,..., r$. Let $\tilde{b}_i$ denote the control influence vector corresponding to the i^{th} damper location, let M denote the $m \times m$ mass matrix, and let K denote the m x m stiffness matrix. The effect of the damper in the structure is modeled as

$$M\ddot{x} + \sum_{i=1}^{r} k_v^i \tilde{b}_i \tilde{b}_i^t \dot{x} + (K + \sum_{i=1}^{r} k_p^i \tilde{b}_i \tilde{b}_i^t)x = f, \tag{2.1}$$

where f represents a forcing function. Next let Φ denote the modal matrix so that $\Phi^t M \Phi = I$ and $\Phi^t K \Phi = D$, with

$$D = diag(\omega_1^2, \omega_2^2 ..., \omega_n^2). \tag{2.2}$$

Set $b_i = \Phi^t \tilde{b}_i$ and let B denote the $n \times r$ matrix with columns b_i. The components of the vector b_i are denoted by superscript, so that $b_i = (b_i^1, ... b_i^n)^t$. Let $K_p = diag(k_p^1, ... k_p^r)$ and $K_v = diag(k_v^1, ... k_v^r)$. The damper parameters are thus encoded in the triple $(B, K_p, K_v) \in$ R ^{nxr} x R^r x R^r.

Next let $J : R^{n\times r} \times R^r \times R^r \to R$ denote the objective functional for the optimization. In subsequent sections J will be taken as either a measure of system level damping, or the H_2 norm of the transfer function between specified inputs and outputs. Let $U \subset R^{n\times r}$ denote the discrete set of possible values of B corresponding to the finite number of locations for distributing the dampers in the structure. To complete the definition of the design space we let $\Omega_{K_p}, \Omega_{K_v} \subset R^r$ denote the admissible values for damper stiffness and dashpot coefficients, respectively.

With this notation, the general optimization problem is posed as

$$\min_{U \times \Omega_{K_p} \times \Omega_{K_v}} J(B, K_p, K_v). \tag{2.3}$$

This paper examines two distinct subproblems associated with the optimization problem above. The first problem derives from fixing the damper locations, i.e., fixing the value of B, and then optimizing the parameters K_p and K_v. This is called the *tuning* problem, In this case the mapping $(K_p, K_v) \to J(B, K_p, K_v)$ will be a smooth map for the choices of J treated

in the paper. " A sequential quadratic programming method is used to solve this optimization problem. Sequential quadratic programming is a method for solving general nonlinear optimization problems with nonlinear constraints (both equality and inequality constraints). It is based on iteratively solving a sequence of quadratic programming subproblems obtained by approximating the cost and constraint functions. These subproblems can also be related to applying a Newton's method for solving the Kuhn-Tucker conditions of the full problem.

In the second problem K_p and K_v are held fixed while the damper locations, B, are optimized. To select r damper locations out of N possible candidate locations (N is the total number of feasible locations in the structure) such that J is optimized, is referred to as the *placement* problem. This is a combinatorial optimization problem whose true optimal solution may only be obtained through an exhaustive search of all possible configurations. Due to the fact that the potential number of candidate locations for placement (N) will typically be large in a large space flexible structures, the total number of combinations, $\frac{N!}{r!(N-r)!}$, becomes exceedingly large. Therefore, it is impractical, if not completely impossible, to conduct an exhaustive search. Thus, instead of finding the optimal solution, a reasonable approach is to find a sub-optimal solution with an acceptable cost.

The simulated annealing method was developed as a heuristic optimization approach to solve combinatorial optimization problems with multiple local minima [6]. The basis of simulated annealing is to occasionally accept nonimproving solutions with a certain diminishing probability, It is these probabilistic jumps that allow the interim solutions in the optimization process to climb out of local minima. This method has been applied to the placement problem [9] successfully where a different performance criterion was used. Our approach follows the algorithm in [9] closely and more details can be found there.

3. Damping of Selected Modes.

Referring to the model (2.1), the eigenvalues of the damped system are given by the zeros of the function $detH(\lambda)$ where

$$H(\lambda) = \lambda^2 I + \lambda B K_v B^t + D + B K_p B^t. \tag{3.1}$$

Now let ξ_k denote the damping introduced into the k^{th} mode due to the parameter selection (B, K_p, K_v). Let λ_k denote the k^{th} eigenvalue. Then

$$\xi_k = \frac{-Re(\lambda_k)}{|\lambda_k|}. \tag{3, 2}$$

The'damping metric that is optimized is of the form $J = g(\xi_1(B, K_p, K_v), \ldots . \xi_n(B, K_p, K-v))$ where g is a smooth function from $R^n + R$ (e.g. g = $\sum_{i \in I} \xi_i$ where I denotes the set of targeted modes.) The first order of business for either the continuous or combinatorial optimization problem is the evaluation of the functional g. The major effort in evaluating this function is to determine the perturbed eigenvalue λ_k, since ξ_k is readily obtained from (3,2). For this purpose a Newton scheme for finding these eigenvalues will be developed. It is based on the following theorem.

Theorem 1. Let b^k denote the vector $(b_1^k, \ldots . b_r^k)^t$. Let $\Sigma(\lambda)$ denote the r x r matrix valued function with ij^{th} entry σ_{ij},

$$\sigma_{ij} \cdot \delta_{ij} \cdot \sum_{l \neq k}^{n} (\lambda^2 + \omega_l^2) k_v^j \quad + \quad k_p^j).$$

(Here δ_{ij} denotes the standard Kronecker delta, i.e., δ_{ij} = 1 if j $= i$, and zero otherwise.) Then in an open dense set of the problem data, λ^* is a zero of $detH(\lambda)$ if and only if λ^* is a zero of the function $f_k(\lambda)$,

$$f_k(\lambda) = (\lambda^2 + \omega_k^2) det\Sigma(\lambda) + [(\lambda K_v + K_p) b^k]^t Adj(\Sigma(\lambda)) b^k,$$

where *Au'j(E)* denotes the adjugate of Σ (the transpose of the matrix of cofactors).

Proof. For $\lambda \# \pm i\omega_j$ the identity

$$H(\lambda) = (\lambda^2 I + D)[I + (\lambda^2 I + D)^{-1} B(\lambda K_v + K_p) B^t]$$

can be shown to hold *generically* with respect to the problem data (i.e., in an open dense subset of the parameter space), For such values of λ the identity

$$det(I_{n\times n} + XY) = det(I_{m\times m} + YX),$$

where X and Y are n x m and m x n matrices, respectively, and $I_{k\times k}$ denotes the k x k identity matrix, leads to

$$detH(\lambda) = det(\lambda^2 I + D) * det[I_{r\times r} + B^t(\lambda^2 I + D)^{-1}B(\lambda K_v + K,)].$$

Let $R = I + B^t(\lambda^2 + D)^{-1}B(\lambda K_v + K_p)$ and let r_{ij} denote its ij^{th} entry, Then

$$r_{ij} = \delta_{ij} + \sum_{l}^{n} \frac{b_i^l b_j^l}{\lambda^2 + \omega_l^2)}(\lambda k_v^j + k_p^j) = \frac{1}{\lambda^2 + \omega_k^2}\{(\lambda^2 + \omega_k^2)\Sigma + b_i^k b_j^k(\lambda k_v^k + k_p^j)\}.$$

Next let V denote the r x r matrix with ij^{th} entry $v_{ij} = b_i^k b_j^k(\lambda k_v^j + k_p^j)$ and observe that

$$det(R) = (\lambda^2 + \omega_k^2)^{-r} det\{(\lambda^2 + \omega_k^2)\Sigma + V).$$

Now since the entries of Σ are rational functions, Σ is defined and invertible everywhere in the complex plane except for finitely many values of λ. Thus except for these values of λ, we have

$$det((\lambda^2 + \omega_k^2)\Sigma + V) = (\lambda^2 + \omega_k^2)^r det(\Sigma) * det(I + \frac{1}{\lambda^2 + \omega_k^2}\Sigma^{-1}V).$$

And since $V = b^k(b^k)^t(\lambda K_v + K_p)$,

$$det((\lambda^2 + \omega_k^2)\Sigma + V) = (\lambda^2 + \omega_k^2)^r det(\Sigma) * \{1 + \frac{1}{\lambda^2 + \omega_k^2}[(\lambda K_v + K_p)b^k]^t\Sigma^{-1}b^k\}.$$

Therefore,

$$\begin{aligned} det(H) &= (\prod_{l\neq k}(\lambda^2 + \omega_l^2))(\lambda^2 + \omega_k^2)det(\Sigma) * \{1 + \frac{1}{\lambda^2 + \omega_k^2}[(\lambda K_v + K_p)b^k]^t\Sigma^{-1}b^k\} \\ &= (\prod_{l\neq k}(\lambda^2 + \omega_l^2))\{(\lambda^2 + \omega_k^2)det(\Sigma) * +[(\lambda K_v + K_p)b^k]^t Adj(\Sigma)b^k]\}. \end{aligned}$$

Since $detH(\pm i\omega_l) \# O$ holds for all l in a dense open subset of the parameter space, on this parameter set $detH$ vanishes precisely when f_k vanishes.///

The function f_k will next be used to determine eigenvalues of the damped system in a neighborhood of the undamped eigenvalue $i\omega_k$. Note that when $K_v = K_p = O$, $f_k(i\omega_k) = O$. This observation combined with the fact that f_k is continuous (even analytic) in a neighborhood of $i\omega_k$, and smooth with respect to the problem data, makes it an excellent function for applying Newton's method for computing the perturbation in the k^{th} eigenvalue resulting from the insertion of damping elements.

The update law for Newton's method to determine the zero of f_k in a neighborhood of $i\omega_k$ is

$$\lambda_k^n = \lambda_k^{n-1} - f_k'(\lambda_k^{n-1})/f_k(\lambda_k^{n-1}), \tag{3.3}$$

where λ_k^n denotes the n^{th} iterate and f_k' denotes the derivative of f_k. The computation of f_k' requires computing the derivative of $Adj(\Sigma)$. $Adj(\Sigma)$ can be efficiently computed without either explicitly computing the matrix of cofactors determinental expansion, or by having to form Σ^{-1} (recall that for Σ invertible, $Adj(\Sigma) = 1/det(\Sigma)\Sigma^{-1}$). This computation is carried out by using the singular value decomposition $\Sigma == UDW$ together with the relationship $Adj(UDW) = W^* Adj(D)U^*$ for U and W unitary and D diagonal. (Note that $Adj(D)$ is easily computed by inspection.) However, an analogous computationally simple and effective means for computing the derivative of the $Adj(\cdot)$ function without resorting to the relationship $Adj(S) = 1/det(S)S^{-1}$ has not been found. The Newton method that is developed is based on this relationship. With this in mind f_k is written as

$$f_k = det(\Sigma)(\lambda_k^2 + \omega_k^2 + [(\lambda K_v + K_p)b^k]^t \Sigma^{-1} b^k]).$$

Although f_k computed in this fashion is not defined at points where Σ is not invertible, it is not difficult to show that the appropriate limits do exist at these points.

To compute f_k' note the following two derivative relationships: (i) $\Sigma^{-1'} = -\Sigma^{-1}\Sigma'\Sigma^{-1}$, and (ii) $(det(\Sigma))' = det(\Sigma)\, tr(\Sigma^{-1}\Sigma')$. The explicit update law for (3.3) is then

$$\lambda_k^n = \lambda_k^{n-1} - h/\{tr(\Sigma^{-1}\Sigma')h + 2\lambda_k^{n-1}$$

$$+([K_v - (\lambda_k^{n-1}K_v + K_p)\Sigma^{-1}\Sigma']b^k)^t \Sigma^{-1} b^k\}, \tag{3.4}$$

where

$$h = (\lambda_k^{n-1})^2 + \omega_k^2 + < (\lambda_k^{n-1}K_v + K_p)b^k, \Sigma^{-1}b^k > .$$

In the event that Σ is not invertible, we can use f_k as defined in Theorem] with a finite ' difference approximation to approximate f_k'. Since f_k is analytic outside of the set $\{\pm i\omega_l\}_{l\neq k}$, finite differences should yield good approximations to f_k'. However, since there are only finitely many values of λ for which Σ is not invertible, (3.4) will be valid everywhere outside this finite set of values.

This evaluation capability is all that is required for the combinatorial optimization problem, For the SQP algorithm it is desirable to have an analytic form of the gradient of the cost functional. That is, we need to compute VJ with respect to the design variables K_p and K_v. (Recall that now B is fixed.) Let $\chi_i, i = 1,..., 2r$ denote these design variables, where the first r elements correspond to the diagonal entries of K_p, and the next r elements correspond to the diagonal entries of K_v. Now write $\lambda_k = u_k + iv_k$. Then we have

$$\frac{\partial g}{\partial \chi_i} = \sum_j \frac{\partial g}{\partial \xi_j}\frac{\partial \xi_j}{\partial \chi_i} \tag{3.5}$$

where

$$\frac{\partial \xi_k}{\partial \chi_i} = \frac{v_k(v_k\frac{\partial u_k}{\partial \chi_i} - u_k\frac{\partial v_k}{\partial \chi_i})}{|\lambda_k|^{3/2}}. \tag{3.6}$$

The partial derivatives of u_k and v_k are the real and imaginary parts of the corresponding partial derivatives of the eigenvalue λ_k.

To obtain the eigenvalue derivative of λ_k, the system (2.1) is placed into the first order form:

$$\dot{x} = Ax + \tilde{f}, \tag{3.7a}$$

where

$$A = \begin{pmatrix} 0 & I \\ -D - BK_pB^t & -BK_vB^t \end{pmatrix} \qquad \tilde{f} = \begin{bmatrix} 0 \\ \Phi^t f \end{bmatrix}. \tag{3.7b}$$

There is a one-to–one correspondence between the solutions to $detH(\lambda) = O$ and the eigenvalue problem $\lambda I - A = O$. Furthermore, if $detH(\lambda_k) = O$ with $H(\lambda_k)\phi_k = O$, it is straightforward to verify that $(\lambda_k - A)\tilde{\phi}_k = O$, where

$$\tilde{\phi}_k = [\phi_k^t \quad \lambda_k\phi_k^t]^t \tag{3.7c}.$$

To compute the eigenvalue derivative of λ_k it is also necessary to have the left eigenvector of

A, $\tilde{\phi}_k^L A = \lambda_k \tilde{\phi}_k^L$. This eigenvector is easily computed to be

$$\tilde{\phi}_k^L = \begin{bmatrix} -D\phi_k - BK_p B^t \phi_k \\ \lambda_k \phi_k \end{bmatrix}^t. \tag{3.8}$$

Applying the standard formula for eigenvalue derivatives (see for example [3]) gives

$$\frac{\partial \lambda_k}{\partial \chi_i} = \frac{\tilde{\phi}_k^L \frac{\partial A}{\partial \chi_i} \tilde{\phi}_k}{\tilde{\phi}_k^L \tilde{\phi}_k}. \tag{3.9}$$

Now all that is required to complete the derivative computation is the eigenvector ϕ_k. This is obtained as follows. We first note (as in the proof of Theorem 1) that $\pm i\omega_k$ is generically not an eigenvalue of $H(\lambda)$. Thus if λ_k denotes the perturbed eigenvalue, we have

$$H(\lambda_k) = (\lambda_k^2 I + D)\{I + (\lambda_k^2 I + D)^{-1} B[\lambda_k K_v + K_p] B^t\}$$

Consequently if ϕ_k is the associated eigenvector, then

$$\phi_k + (\lambda_k^2 I + D)^{-1} B[\lambda_k K_v + K_p] B^t \phi_k = 0, \tag{3.10}$$

and for any vector x

$$< \phi_k \ , x >= - < \ (\lambda_k^2 I + D)^{-1} B[\lambda_k K_v + K_p] B^t \phi_k, x >.$$

Multiplying (3. 10) on the left by B^t shows that $B^t \phi_k$ solves the equation

$$\psi + B^t (\lambda_k^2 I + D)^{-1} B[\lambda_k K_v + K_p] \psi = 0. \tag{3.11}$$

These observations motivate the following

Proposition 2. Suppose B has full rank. Then there is a one-to-one correspondence between the independent solutions of equations (3.10) and (3.11) given by

$$\psi = B^t \phi, \tag{3.12}$$

and

$$\phi = -(\lambda_k^2 I + D)^{-1} B(\lambda_k K_v + K_p)\psi. \tag{3.13}$$

In particular, the eigenvectors of the perturbed system corresponding to the eigenvalue λ_k (or equivalently, the nullspace of $H(\lambda_k)$), can be obtained via the solutions of (3.1 1) toget her with (3.13).

Proof. It has already been shown that if ϕ is in the nullspace of $M(\lambda_k)$ then $B^t\phi_k$ satisfies (3.1 1). Conversely, suppose ψ solves (3.11). Then $\psi = B^t\phi$ where ϕ is defined as

$$\phi = -(\lambda_k^2 I + D)^{-1} B(\lambda_k K_v + K_p)\psi.$$

And since $\psi = B^t\phi$, it follows that #J solves (3.10) and is in the nullspace of $H(\lambda_k)$.

To show that the correspondence between solutions is one-to-one, note first that since B has full rank, the matrix $(\lambda_k^2 I + D)^{-1} B(\lambda_k K_v + K_p)$ has trivial nullspace, so that if $\psi_1, \ldots$ ...4P are independent solutions of (3.11), then the associated vectors $\phi_1, \ldots . \phi_p$ are independent solutions of (3.10). To prove the result in the opposite direction suppose that ϕ_1 and ϕ_2 are independent solutions of (3.10) with $B^t\phi_1 = \gamma B^t\phi_2$ and γ a nonzero scalar (and thus leading to dependent ψ_i in (3.12)). Inserting these solutions into (3.10) and taking their difference leads' to $\phi_1 = \gamma\phi_2$, a contradiction. Thus $B^t\phi_1$ and $B^t\phi_2$ are independent, completing the proof of the proposition.///

In summary, the function $J = g(\xi_1(B, K_p, K_v), \ldots . \xi_n(B, K_p, K_v))$ and its gradient are computed as follows:

(i) Apply the Newton iteration (3.4) to obtain λ_i, $i \in I$, where I denotes the set of target indices,

(ii) Use (3,2) to obtain ξ_i, i $\in I$.

(iii) Evaluate $g(\xi_i, \ldots . \xi_n)$ using (ii) and the definition of g.

To obtain VJ with respect to $\chi = [diag(K_p)\, diag(K_v)]^t$:

(iv) Solve (3.1 1) to obtain ψ_i

(v) Use (3.13) followed by (3,8) to obtain $\tilde{\phi}_i$ and $\tilde{\phi}_i^L$

(vi) Compute $\partial A/\partial\chi_i$ from (3.7b).

(vii) Apply (3,9) followed by (3.6) and then (3.5) to obtain Vg.

4. $\mathcal{H}_2$ Optimization

The $\mathcal{H}_2$ cost optimization problem is formulated to optimize specific input-output relationships. These relationships are connected to the dynamical equation (2.1) via the system

$$\dot{x} = Ax + B_d f, \tag{4.1a}$$

$$y = Cx. \tag{4.1b}$$

Here A is defined as in (3.7), and

$$x = \begin{bmatrix} q \\ \dot{q} \end{bmatrix}, \quad B_d = \begin{bmatrix} 0 \\ \hat{B}_d \end{bmatrix},$$

where the vector q represents modal coordinates and $\hat{B}_d$ is the disturbance input influence matrix. The objective is to minimize the $\mathcal{H}_2$ norm of the transfer function from the input f to the output y. The spectral content of the disturbance input can be shaped, but for simplicity a white noise input is assumed. The $\mathcal{H}_2$ cost is then given by [5]

$$J(B, K_p, K_v) = tr(CC^tQ), \tag{4.2a}$$

where Q solves the Lyapunov equation

$$AQ + QA^T + B_d B_d^t = O. \tag{4.2b}$$

To effectively solve (4.2) as part of an optimization loop requires a significant reduction in its size.

To motivate the method that is used for reducing (4.2), recall that [5]

$$tr(C^tCQ) = \int_0^\infty |G(t)|^2 dt,$$

where $G(t)$ is the impulse response of the system,

$$G(t) = Ce^{At}B_d.$$

Now $e^{At}B_d$ is the response of (4.1) to the input $f(t) = \delta^M(t)$, where $\delta^M(t)$ denotes the matrix comprised of Dirac delta functions in each of the system's input channels. In the forced mode technique [4] improved transient response approximation for systems of the form

$$M\ddot{x} + Kx = f(t)$$

is attained by augmenting a reduced modal model with the Ritz vector K-l f. Furthermore, analysis and empirical studies in [1] reveal that the forced mode method is also effective for obtaining high fidélity reduced models for the system (2.1). We are led to include Ritz vectors (force modes) to statically correct each of the forcing inputs, both the "control" inputs corresponding to the dampers and the disturbance inputs associated with the influence matrix B_d. A reduced model is obtained by pre-multiplying and post-multiplying (2.1) by the matrix l',

$$T = [\Phi_r : K^{-1}B : K^{-1}B_d], \tag{4.3}$$

where Φ_r denotes the matrix comprised of the first m eigenvectors of the nominal system.

For computational purposes it is desirable for T to be M-orthonormal. So let P denote the matrix obtained from T by orthonormalizing its columns. Then in first order form the system (4,1) reduces to

$$\text{x} = A^m x + B_d^m f, \tag{4.4 CL}$$

$$y = C^m x, \tag{4.4b}$$

where

$$A^m = \begin{bmatrix} 0 & I \\ -D_m - P^t B K_p B^t P & -P^t B K_v B^t \end{bmatrix},$$

$$B_d^m = \begin{bmatrix} 0 \\ P^t B_d \end{bmatrix}, \quad C^m = CP,$$

and $D_m = diag(\omega_1^2, \ldots . \omega_m^2)$ where r = m+ number of input force vectors.

An approximation to the cost functional (4.2) is computed as follows:

(i) Form the matrix T in (4.3).

(ii) Orthonormalize its columns with respect to the mass matrix M.

(iii) Form the matrices Am, B_d^m, and Cm in (4.4).

(iv) Solve (4.2b) with A and B_d replaced with Am and B_d^m, respectively.

(v) Evaluate (4.2a) with C replaced by Cm

5. Numerical Examples

A detailed description of the JPL testbed can be found in [7] (see Figure 1). Briefly, the system is modeled with 249 degrees of freedom and contains 186 candidate locations to insert damping devices. This study is restricted to placing and tuning three viscous dampers. The stiffness of these dampers can vary between 8,000 lbs/in and 100,000 lbs/in, and the damping coefficients have bounds $0 \leq k_v \leq 1000$ lbs-sec/in. To obtain the correct K_p in (2.1), it is necessary to use the value that is the difference between the damper stiffness and the truss element it replaces.

Because the accuracy of the cost functional evaluation methods is of paramount importance, Table 1 contains a comparison of eigenvalue approximations using the full order model, the Ritz reduced model, a modally reduced model, and the Newton method. The first column in the table contains these values for the undamped nominal system. All of the other values correspond to the damped system after three viscous dampers are inserted into the structure. (The placement as shown in Table 1 was obtained by optimizing the sum of damping coefficients in the first seven modes of the system. This will be discussed more below.) The conclusion here is that the Ritz reduction technique and the Newton iteration yield high precision estimates with enormous reduction in operation count, while the modally reduced model produces inaccurate results.

What is of equal significance is that not only does the modally reduced model produce inaccurate results, it also leads to inaccurate trends for choosing damper parameters. Figure 2 contains damping predictions of the second system mode as a function of the damper viscous parameter coefficient. Note that the full and Ritz reduced models lead to an optimal coefficient of approximately 500 lbs-sec/in, while the modally reduced model leads to a significantly larger value that is very suboptimal. The Ritz reduction method also leads to very accurate approximations to solutions to the Lyapunov equation (4.2b) via the substitutions outlined in Step (iv). The Ritz approximation provided six digits of accuracy for the solution of the Lyapunov equation.

Table 2 contains the eigenvalues of two damped systems where the damper locations were

chosen by the simulated annealing process to optimize in the first case an $\mathcal{H}_2$-norm, and in the second case a direct metric of the damping. For both optimization problems the simulated annealing process was initiated by using 20 randomly chosen combinations to obtain an initial temperature (energy) by first computing the average energy variations among these initial 20 configurations. This value is divided by 0.4 to yield a 67% probability for accepting nonimproving solutions initially. The "temperature" is then reduced by a factor of 0.8 successively until convergence is reached. More details on the entire' process and the selection of these parameters can be found in [9]. The optimal placement of the dampers for these solutions are shown in Figure 3. The first set of eigenvalues corresponds to optimizing the placement with respect to the $\mathcal{H}_2$ norm of the transfer function from an input disturbance located at grid point 412 between the third and fourth bays of the structure, and outputs consisting of all of the nodal displacements di rectly beneath the trolley (see Fig. 1). The disturbance was generated as the output of a 6^{th} order low–pass filter with a bandwidth of 25 Hz. This choice of weighting function reflects the objective of damping disturbances in the frequency range below 25 Hz. The second set of eigenvalues results from placing the dampers to optimize the sum of the damping in the system modes below 25Hz. A comparison of the respective Bode plots of the resulting transfer functions is also given in Figure 3. As observed from Table 2 and Figure 3, large damping is introduced into the second and third modes as a result of optimizing the damping. However, this is at a sacrifice to the damping attained attained in the other modes. The $\mathcal{H}_2$ norm optimization metric distributes the damping across the modes in a much more even fashion.

The next example illustrates how particular modes can be targeted for damping. The objective in this example is to achieve maximal damping in modes 5,6, and 7 without sacrificing darnping in any one of them. A metric of this type is useful when used in conjunction with control design. For example, if a certain controller bandwidth is selected, then damping modes in the loop gain crossover frequency region is highly desired. A minimax optimization problem is appropriate for this objective, i.e. maximize the minimal damping achieved in the fifth, sixth, and seventh modes. A two step procedure consisting of first choosing the damper locations followed by optimizing their parameters was implemented. A smooth cost

functional approximation to the minimax problem was used:

$$9 = \sum_{i=5}^{7} exp(\mu \xi_i),$$

wit μ representing a "{large" parameter. This choice of cost functional can be rigorously justified as an approximation to the minimax problem [8]. We first fixed the stiffness and dashpot values to $k_p = 8000 lbs/in$ and $k_v = 320 lbs - see/in$, and optimized the damper locations via simulated annealing with respect to the metric above. With the new damper locations, the parameters of the dampers were optimized with respect to the approximate minimax metric using the SQP algorithm. (We used the NPSOL package developed at the "Systems Optimization Laboratory at Stanford University for the SQP algorithm.) The damper locations and system damping values (both before and after tuning the damper parameters) are shown in Figure 4. The strategy located the dampers near the "arm" of the testbed. As can be seen considerable damping is added to the targeted modes over the "optimal" locations obtained for either the sum of damping metric or the H_t metric. Also note that after the dampers are tuned, the damping in modes 6 and 7 are more than doubled at the expense of about a 2070 decrease in damping in mode 5.

6. Concluding Remarks

The use of strategically placed damping elements in future large space structures will play a significant role in their design and development, The ability to analyze, predict, and ultimately optimize system responses with respect to these passive devices is critical for the application of this technology.

Several aspects and approaches to carrying out the analysis of these problems were discussed in the paper. The fundamental ingredient in each of these problems is the choice of performance functional and its evaluation. Because these systems are typically prohibitively large for direct functional evaluation, alternative solutions are necessary. In the paper accurate and efficient methods were introduced for functional and gradient evaluation, including a Ritz reduction technique and a Newton algorithm. We also presented an example where

straightforward modal reduction led to very erroneous results,

The results of the paper indicate that significant levels of damping can be introduced into these structures in a very systematic and tailored manner,

Acknowledgments

The research described in this paper was carried out by the Jet Propulsion Laboratory, California Institute of Technology, under a contract with the National Aeronautics and Space Administration.

References

1. Chu, C.C. and Milman, M., "Eigenvalue Error Analysis of Viscously Damped Structures Using a Ritz Reduction Method," *AIAA Journal,* Vol 30, pp 2935-2944, Dec. 1992.

2. Gill, P. E., Murray, W., and Wright, M., *Practical Optimization,* Academic press Inc., San Diego, CA, 1989.

3. Golub, G. H., and Van Loan, C. F., *Matrix Computations,* The Johns Hopkins University Press, Baltimore, MD, 1989.

4. Gu, K. and Tongue, B. H., "A Method to Improve the Modal Convergence for Structures with External Forcing," *Journal of Applied Mechanics,* Vol. 54, pp. *904-909, Dec., 1987.*

5. Kwakernaak, H., and Sivan, R., *Linear Optimal Control Systems,* John Wiley and Sons, New York, New York, 1972.

6. Kirkpatrick, S., Gelatt, C. D., and Vecchi, M. P., "Optimization by Simulated Annealing," Science, Vol. *22,* pp. 671-680, May, 1983.

7. O'Neal, M., Eldred, D., Liu, D., and Redding, D., "Experimental Verification of Nanometer Level Optical Pathlength Control on a Flexible Structure," *14th Annual A AS Guidance and Control Conference,* Keystone, CO, Feb., 1991.

8. Polyak, A., "Smooth Optimization Methods for Minimax Problems," *SIAM J. Control and Optimization, 26,* pp. 1274-1286, Nov., 1988.

9. Chen, G.-S., R.J. Bruno, M. Salama, "Optimal Placement of Active/Passive Elements in Truss Structures Using Simulated Annealing," *AIAA Journal,* Vol. 29, pp.1327-1334, Aug., 1991.

10. Yiu, Y. C., "System Level Design and Analysis of Truss Structures Damped by Viscous Struts," *Damping '91 Conference,* San Diego, CA, Feb., 1991.

11. Chang, M. I. J., and Soong, T. T., "Optimal Controller Placement in Modal Control of Complex Systems," *Journal of Mathematical Analysis and Applications,* Vol. 75, 1980, pp. 340-358.

12. Chu, C. C., Fanson, J., Milman, M., and Eldred, D., "Optimal Active Member and Passive Damper Placement and Tuning," *Proceedings of 4th NASA/DoD Control/Structures Interaction Technology Conference,* Orlando, FL, Nov. 5-7, 1990.

13. Haftka, R., and Adelman, H., "Damping and Control of Spacecraft Structures: Selection of Actuator Location for Static Shape Control of Large Space Structures by Heuristic Integer Programming," *Computers and Structures,* Vol. 20, Nos. 1-3, 1985, pp. 575-582.

14. De Lorenzo, M. L., "Sensor and Actuator Selection for Large Space Structures," *Journal of Guidance, Control, and Dynamics,* Vol. 13, pp. 249-257, March–April, 1990.

15. Hu, A., Skelton, R, E., Norris, G. A., and Corssey, D. F., "Selection of Sensors and Actuators with Applications to the ASTREX Facility," *Proceedings of 4th NASA/DoD Control/Structures Interaction Technology Conference,* Orlando, FL, Nov. 5-7, 1990.

16. Wu, Y. W., Rice, R. B., and Juang, J. N., "Sensor and Actuator Placement for Large Flexible Space Structures," *Proceedings of the Joint Automatic Control Conference,* Denver, CO, June 1979.

17. Johnson, T. L., "Principles of Sensor and Actuator Location in Distributed Systems," *Proceeding of NCKU/AAS International Symposium on Engineering Sciences and Mechanics,* Tainan, Taiwan, Dec 1981.

18, Juang, J. N. and Rodriguez, G., "formulations and Applications of Large Structure Actuator and Sensor Placements," *Second VPI and SU/AIAA Symposium on Dynamics and Control of Large Flexible Spacecraft,* June, 1979.

Mode	Undamped System	Damped System with 3 Dampers at Location 132, 140, 142 (k_v = 8,000 lb/in, k_v = 320 lb/in)			
	Frequency (Hz)	Frequency Hz)			
		249 Modes (Full order)	12 Modes plus 3 Ritz Vectors	Newton Method	15 Modes (Truncation)
1	0.7427	0.7420	0.7420	0.7420	0.7425
2	5,4263	5.2940	5.2940	5.2940	5.3262
3	7.4565	7.0376	7.0376	7.0376	6.9540
4	11.6777	10,4862	10.4862	10.4862	10.4493
5	17.4248	17.4386	17.4386	17.4386	17.3444
6	20.8423	20.8236	20.8236	20.8236	20.7055
7	31.1387	31.2231	31.2231	31.2231	31.0481

Table 1 (a)

Comparison of Modal Frequencies and Dampings (Frequencies)

Mode	Damped System			
	Damping (%)			
	249 Modes *(Full order)*	12 Modes *plus* 3 Ritz Vectors	Newton Method	15 Modes *(Truncation)*
1	0.0179	0.0179	0.0179	0.0012
2	4.5744	4.5744	4.5744	0.6125
3	25.5358	25.5357	25.5358	2.3228
4	32.6380	32.6379	32.6380	5.5664
5	0.9033	0.9034	0.9033	0.4066
6	1.3197	1.3197	1.3197	0.5709
7 “	0.5013	0.5016	0.5013	0.5031

Table l(b)

Comparison of Modal Frequencies and Dampings (Dampings)

Mode	Damper Locations			
	$\mathcal{H}_2$-Norm Optimized (6, 19, 91)		Dampings Optimized (132, 140, 142)	
	Frequency (Hz)	Damping (%)	Frequency (Hz)	Damping (%)
1	0.7414	0.0245	0.7420	0.0179
2	5.0393	6.8905	5.2940	4.5744
3	7.1748	10.0192	7.0376	25.5358
4	11.4717	3.7751	10.4862	32.6380
5	17.5924	3.2823	17.4386	0.9033
6	20.9413	2.0084	20.8236	1.3197
7	31.1573	*0.0788*	31.2231	0.5013

Table 2.

Comparison of Damped Eigenvalues

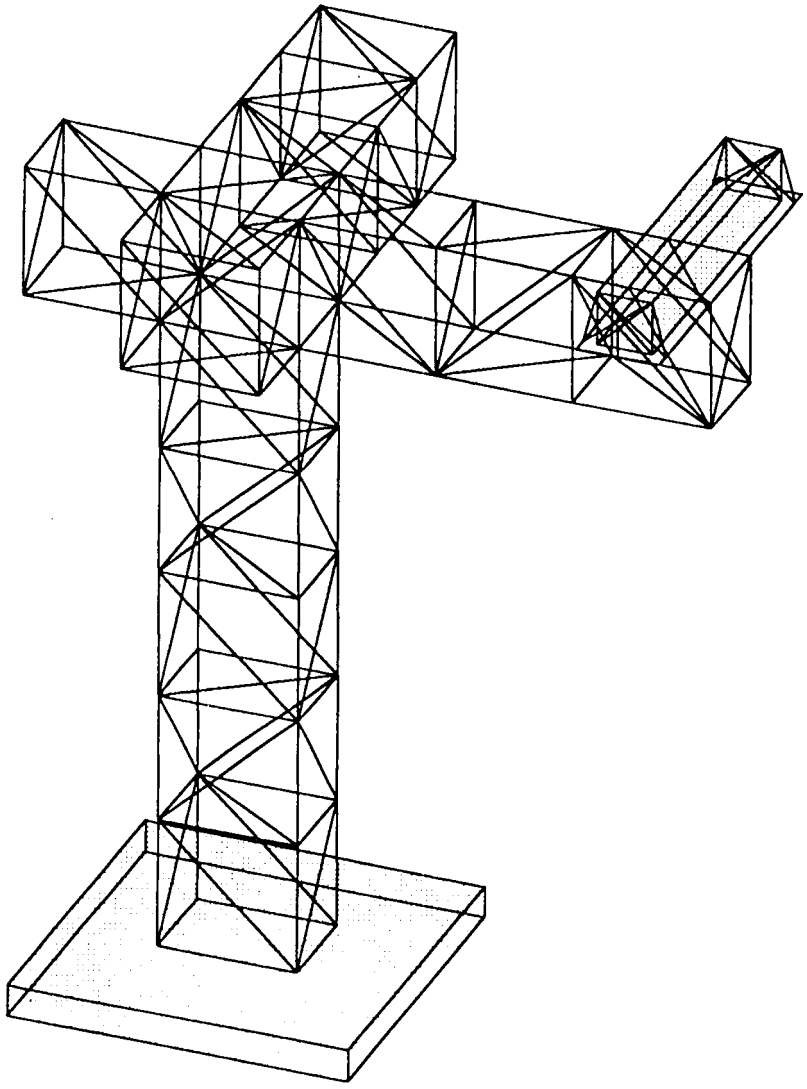

Figure 1.
JPL CSI Phase B Testbed

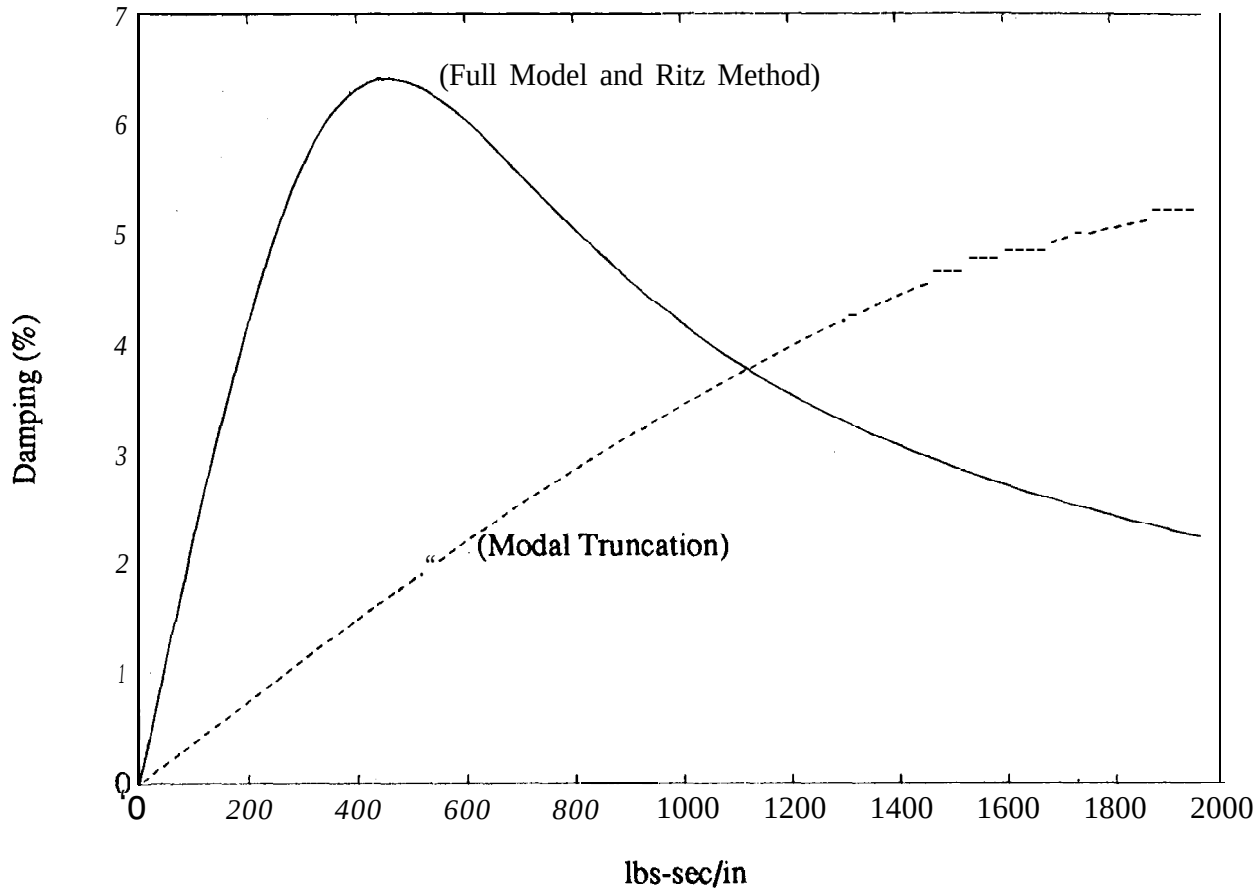

Figure 2.

Damping Prediction by Reduction Methods

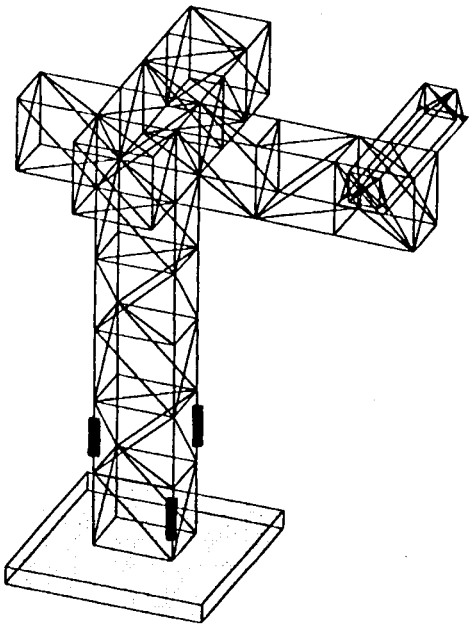

Sum of Damping Optimized

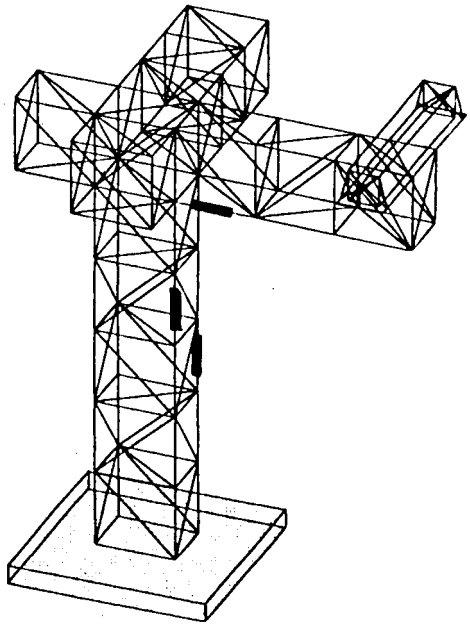

$\mathcal{H}_2$-Optimized

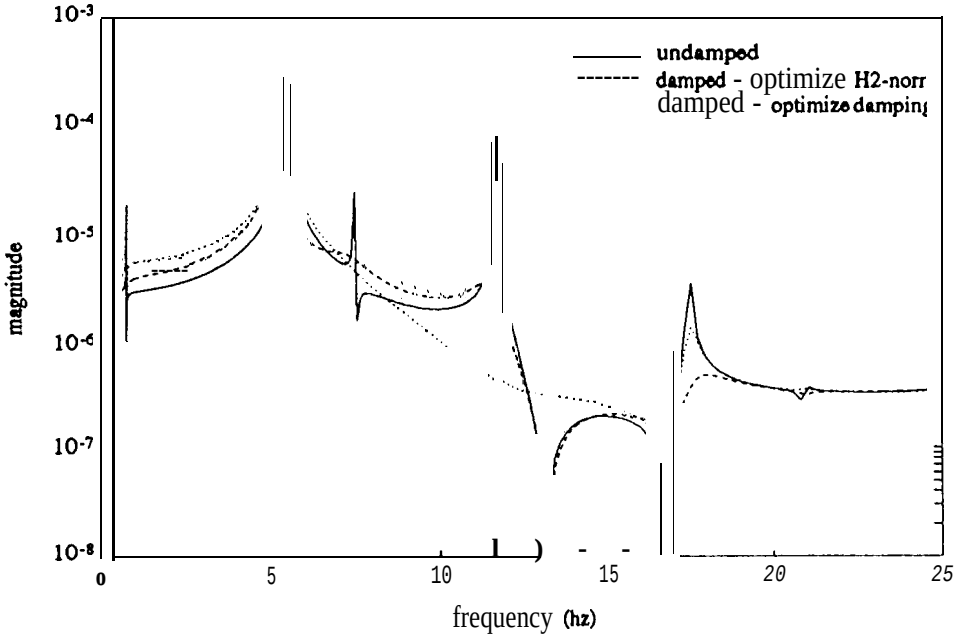

Figure 3.
Frequency Responses of Undamped and Damped Systems

Mode	Undamped Frequency (Hz)	Not Tuned Frequency (Hz)	Not Tuned Damping (%)	Tuned Frequency (Hz)	Tuned Damping (%)
5	17.4248	17.2668	8.1733	16.1907	6.5787
6	20.8423	21.3353	3.9098	20,1644	8.0746
7	31.1387	32.1426	3.7256	30.5854	7.4840

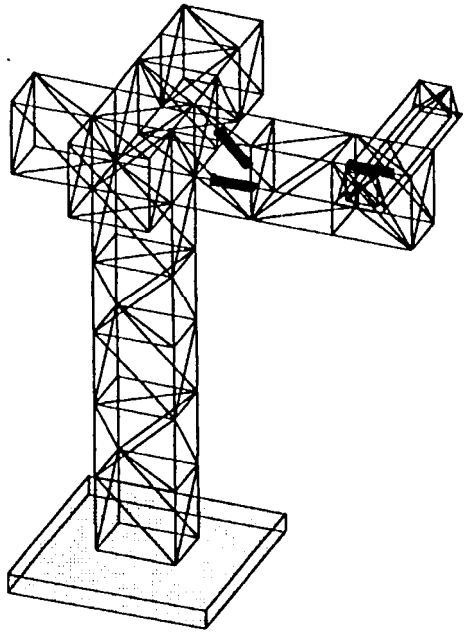

Figure 4.
Minimax Optimized Placement and Tuning